Electronic Supplementary Material (ESI) for RSC Advances.

Supporting Information

A highly sensitive benzimidazole-based chemosensor for the colorimetric detection of Fe(II) and Fe(III) and the fluorometric detection of Zn(II) in aqueous media

Yong Sung Kim, Jae Jun Lee, Sun Young Lee, Tae Geun Cho, Cheal Kim*

Department of Fine Chemistry, Seoul National University of Science and Technology, Seoul 139-743, Korea.
Fax: +82-2-973-9149; Tel: +82-2-970-6693; E-mail:chealkim@seoultech.ac.kr

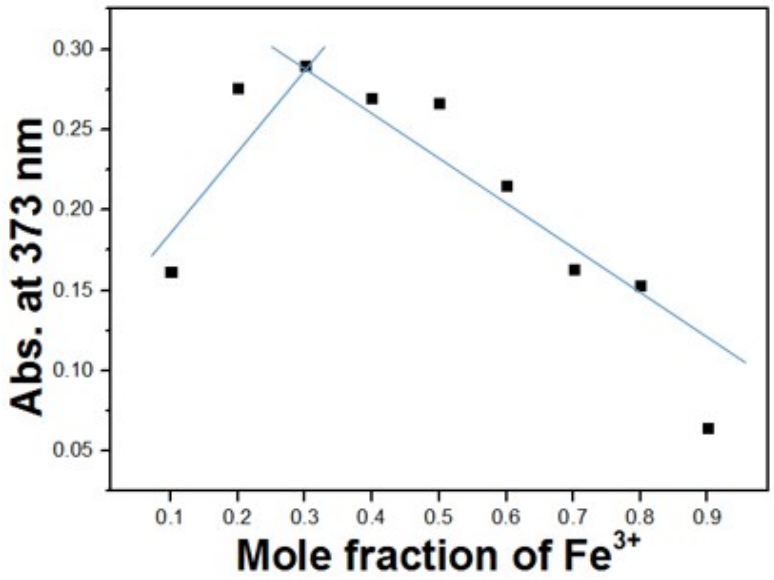

Figure S1. Job plot for the binding of **1** with Fe^{3+}. Absorbance at 373 nm was plotted as a function of the molar ratio **1** with Fe^{3+}. The total concentration of Fe^{3+} ions with receptor **1** was 70 μM.

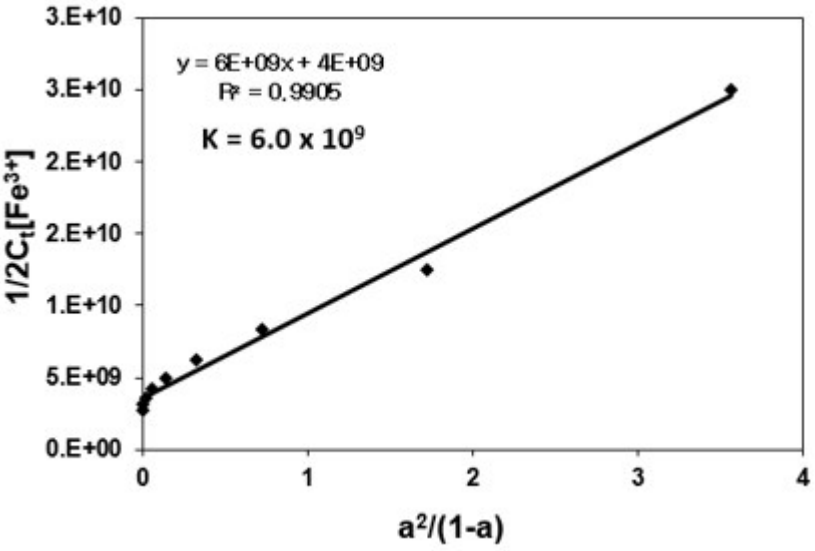

Figure S2. Li's plot (absorbance at 445 nm) of **1** (20 μM), assuming 2:1 stoichiometry for association between **1** and Fe^{3+}.

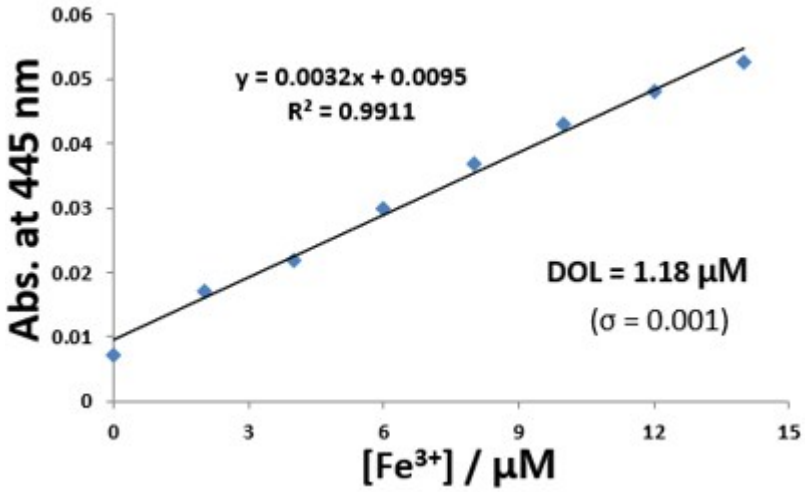

Figure S3. Determination of the detection limit based on change in the ratio (absorbance at 445 nm) of **1** (20 μM) with Fe^{3+}.

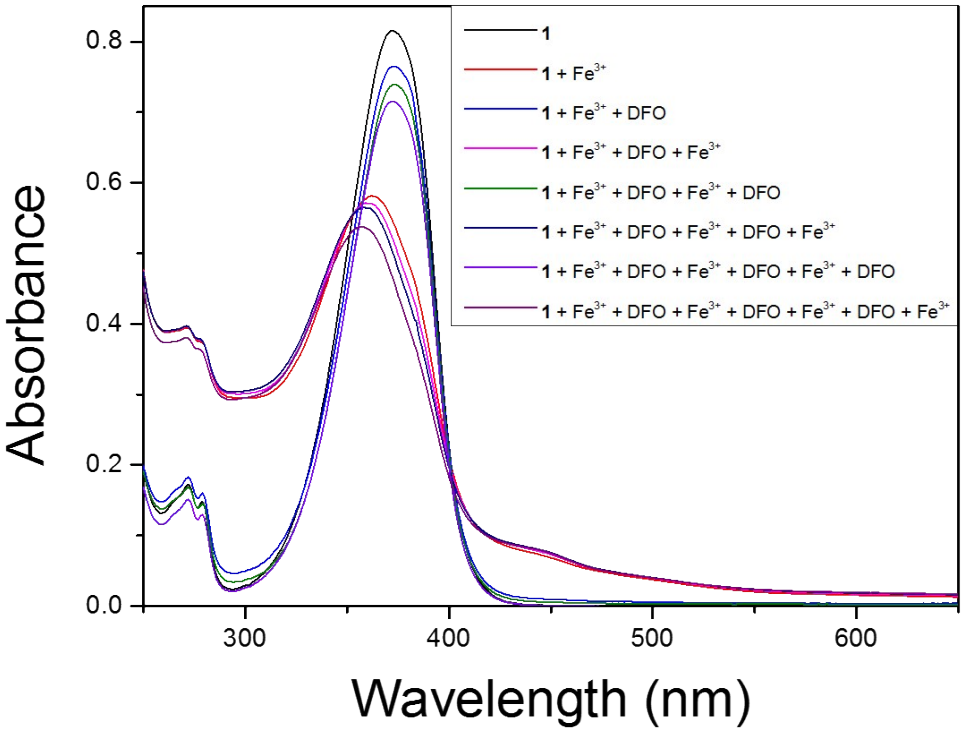

Figure S4. UV-vis spectral changes of **1** (20 μM) after the sequential addition of Fe^{3+} and DFO**.**

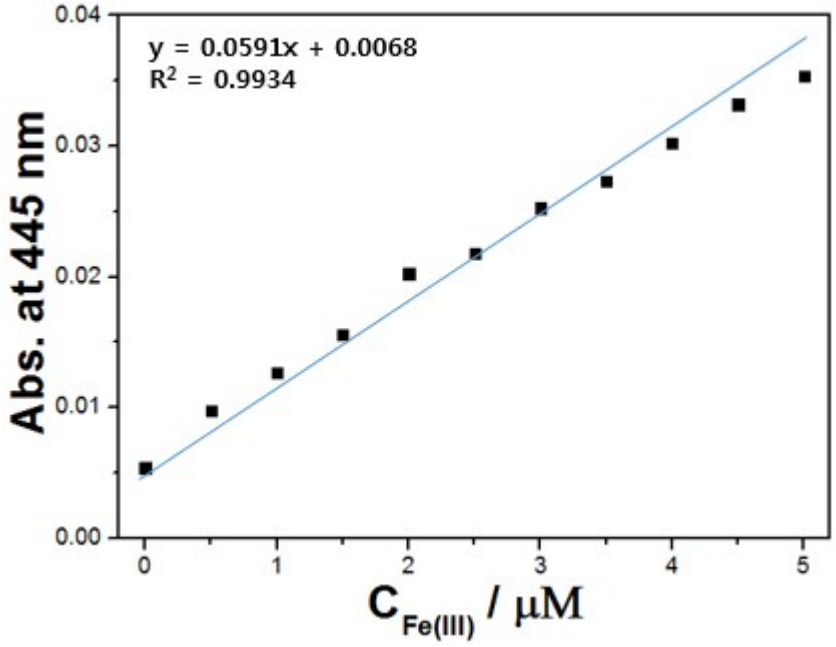

Figure S5. Absorbance (at 445 nm) of **1** as a function of Fe(III) concentration. [**1**] = 10 μmol/L and [Fe(III)] = 0.00-5.00 μmol/L. Conditions: all samples were conducted in bis-tris buffer solution (10 mM, pH 7.0).

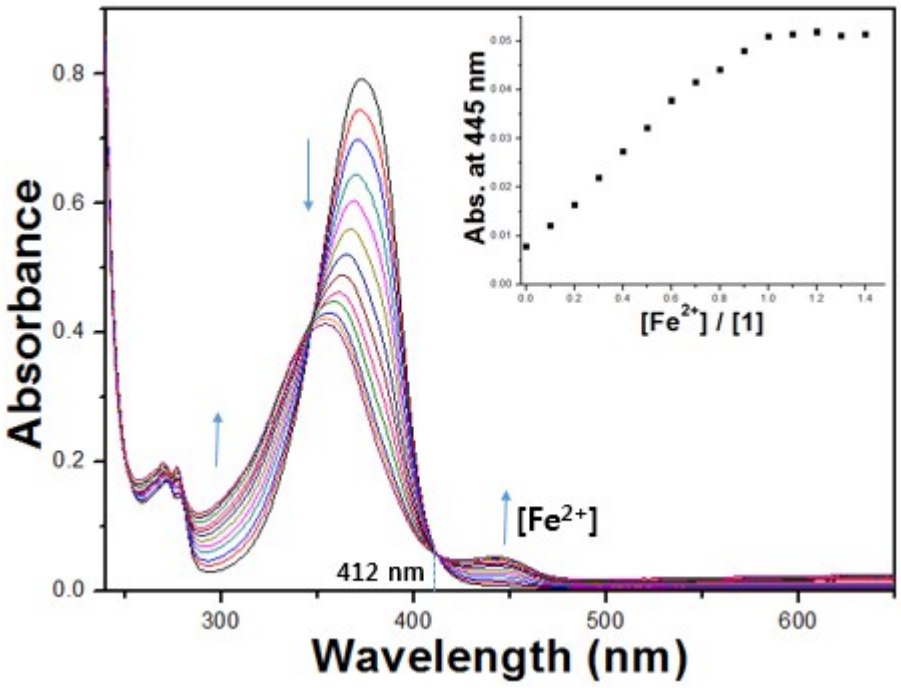

Figure S6. UV-vis spectra of receptor **1** (20 μM) upon the addition of different concentrations of Fe^{2+} in bis-tris buffer solution (10 mM, pH 7.0). Inset: absorption at 445 nm versus the number of equiv of Fe^{2+} added.

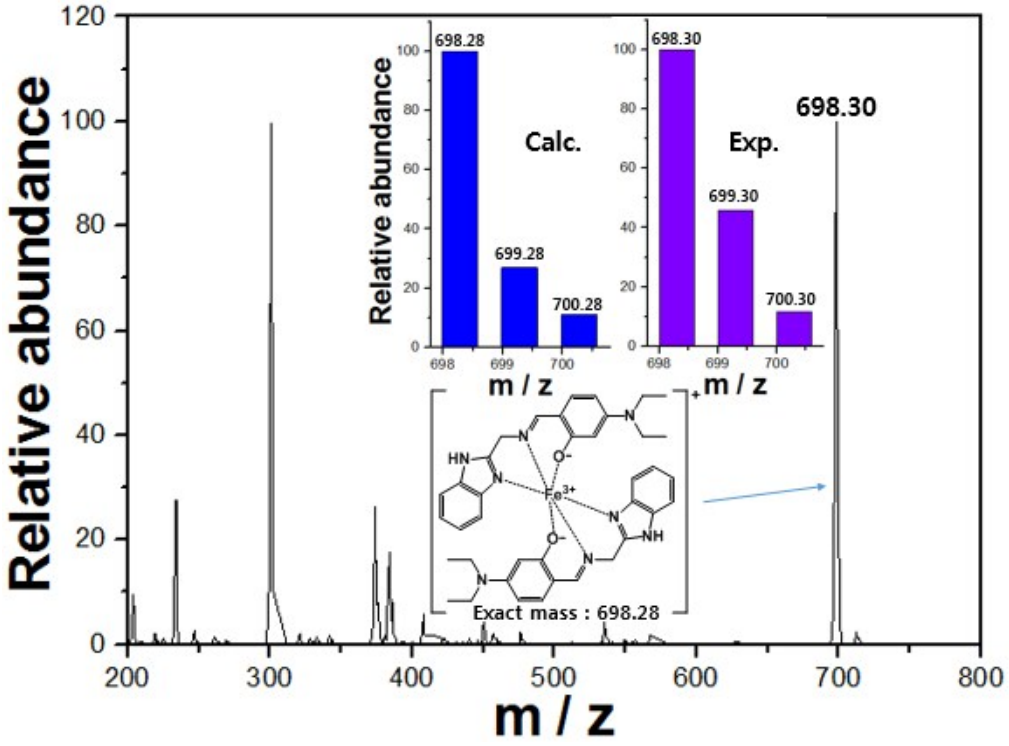

Figure S7. Positive-ion electrospray ionization mass spectrum of **1** (0.1 mM) upon addition of Fe^{3+} (0.1 mM).

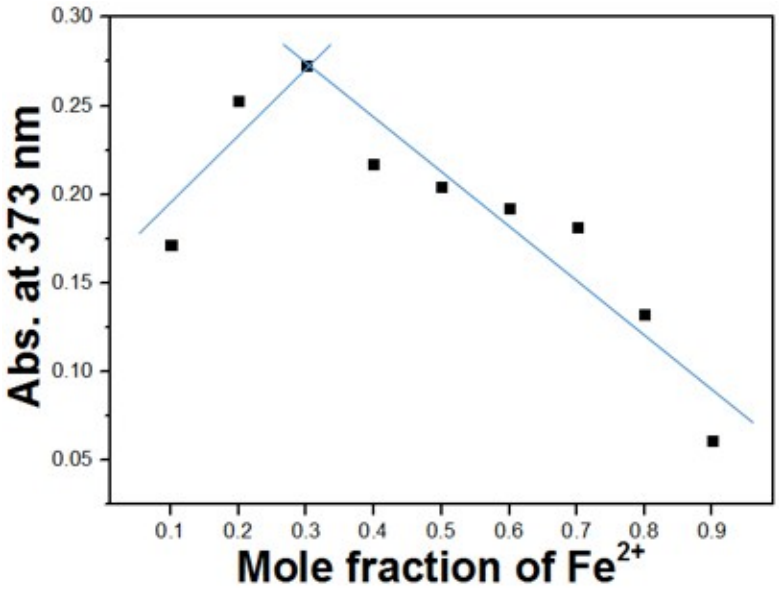

Figure S8. Job plot for the binding of **1** with Fe^{2+}. Absorbance at 373 nm was plotted as a function of the molar ratio **1** with Fe^{2+}. The total concentration of Fe^{2+} ions with receptor **1** was 70 μM.

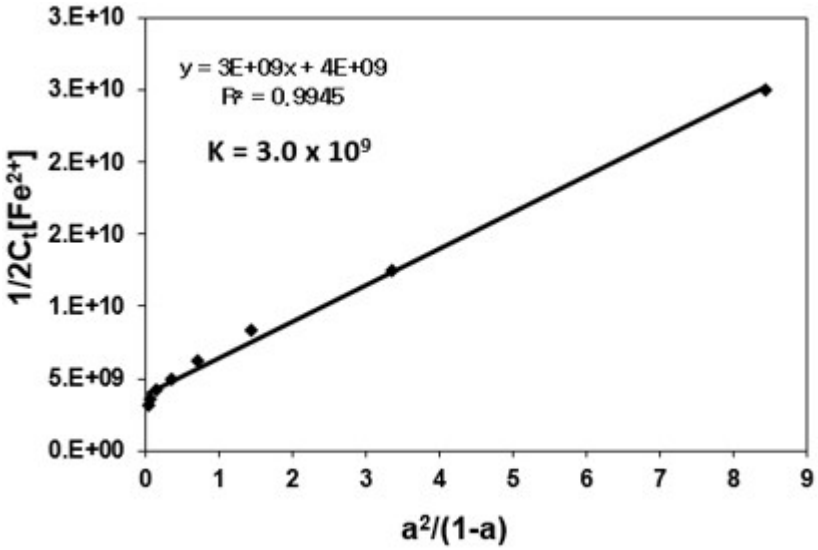

Figure S9. Li's plot (absorbance at 445 nm) of **1** (20 μM), assuming 2:1 stoichiometry for association between **1** and Fe^{2+}.

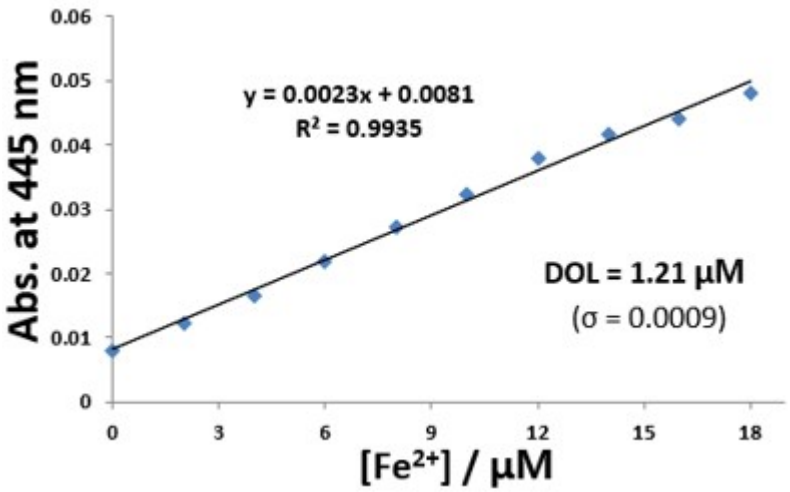

Figure S10. Determination of the detection limit based on change in the ratio (absorbance at 445 nm) of **1** (20 µM) with Fe^{2+}.

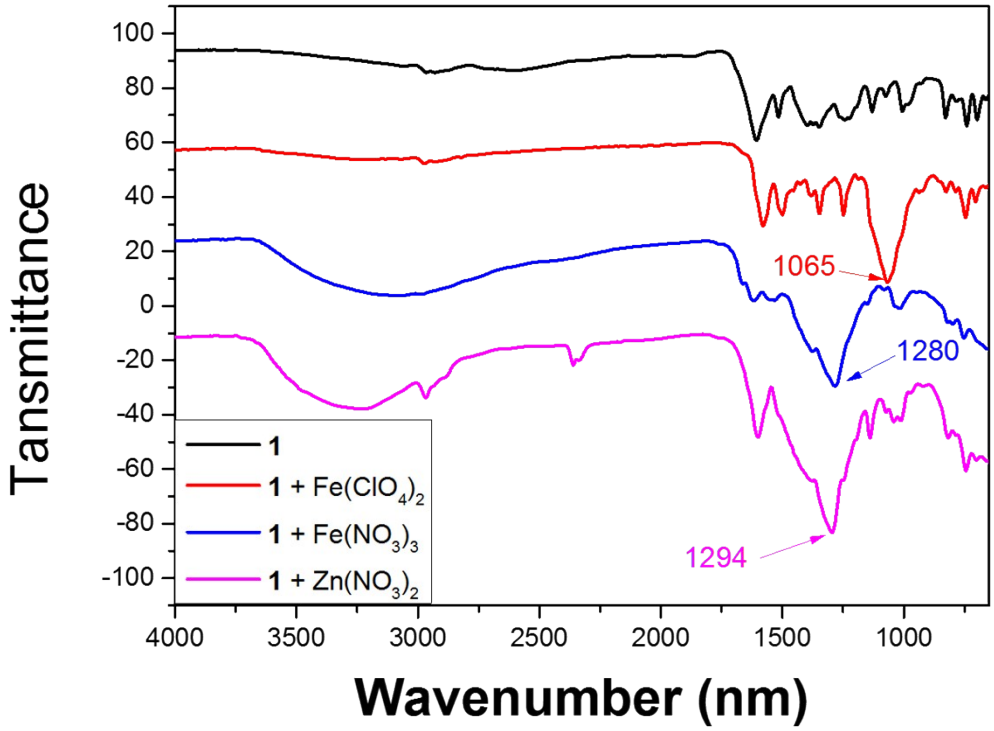

Figure S11. FT-IR spectra of **1**, Fe^{2+}-2·**1**, Fe^{3+}-2·**1** and Zn^{2+}-2·**1** species.

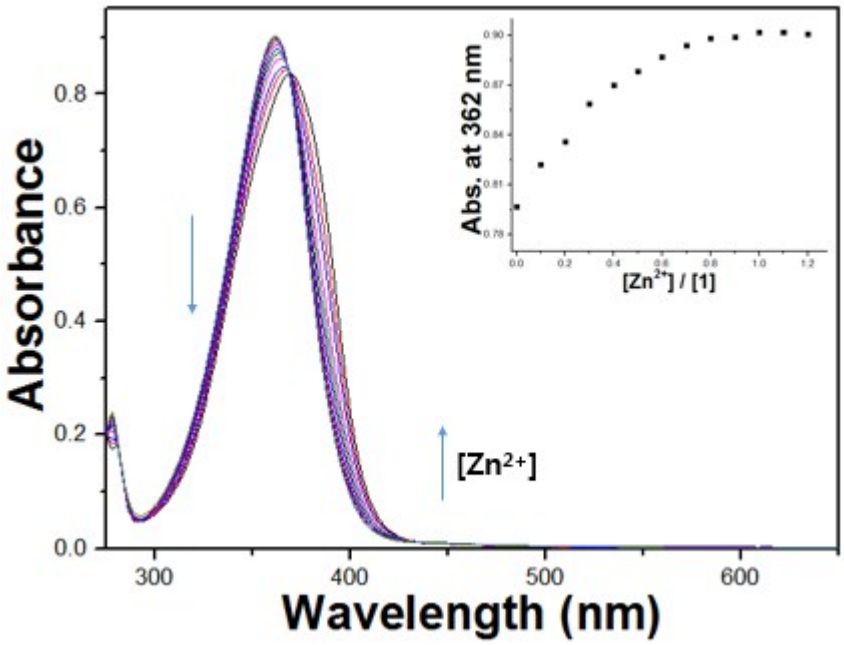

Figure S12. UV-vis spectra of receptor **1** (30 μM) upon the addition of different concentrations of Zn^{2+} in bis-tris buffer solution (10 mM, pH 7.0). Inset: absorption at 362 nm versus the number of equiv of Zn^{2+} added.

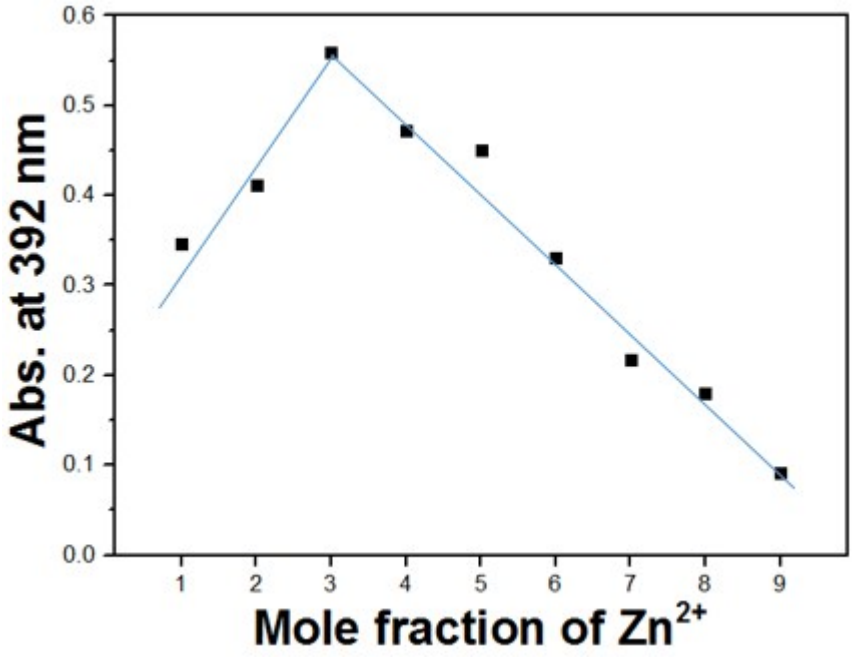

Figure S13. Job plot for the binding of **1** with Zn^{2+}. Absorbance at 392 nm was plotted as a function of the molar ratio **1** with Zn^{2+}. The total concentration of Zn^{2+} ions with receptor **1** was 60 μM.

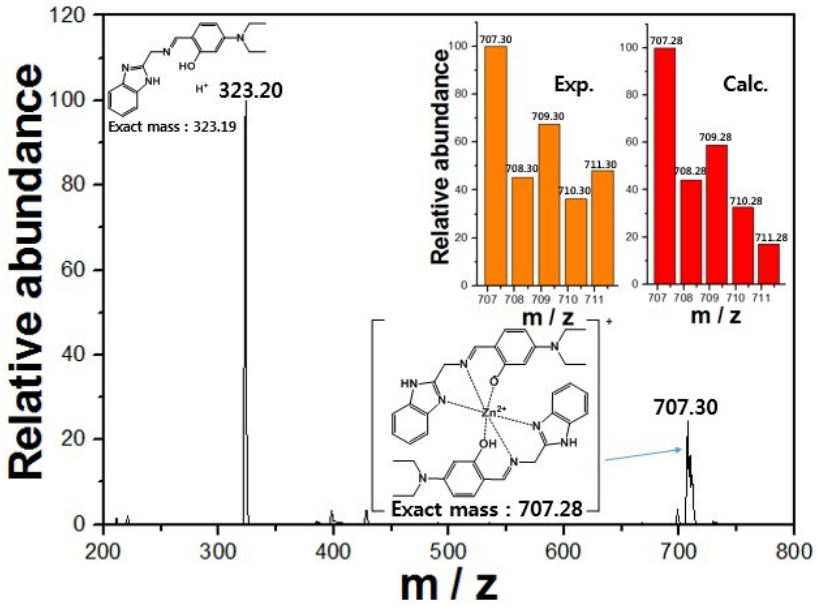

Figure S14. Positive-ion electrospray ionization mass spectrum of **1** (0.1 mM) upon addition of Zn^{2+} (0.1 mM).

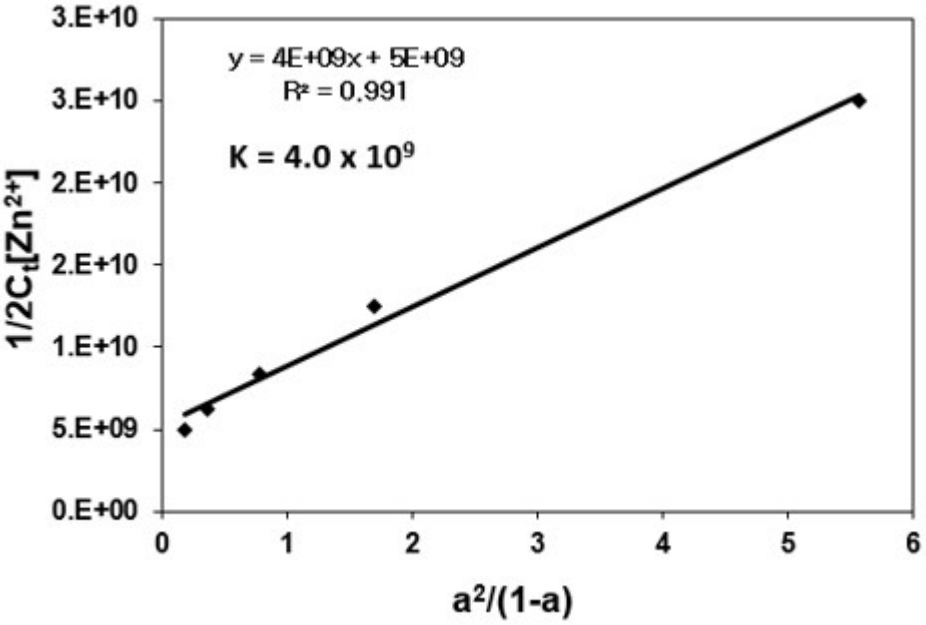

Figure S15. Li's plot (intensity at 425 nm) of **1** (20 μM), assuming 2:1 stoichiometry for association between **1** and Zn^{2+}.

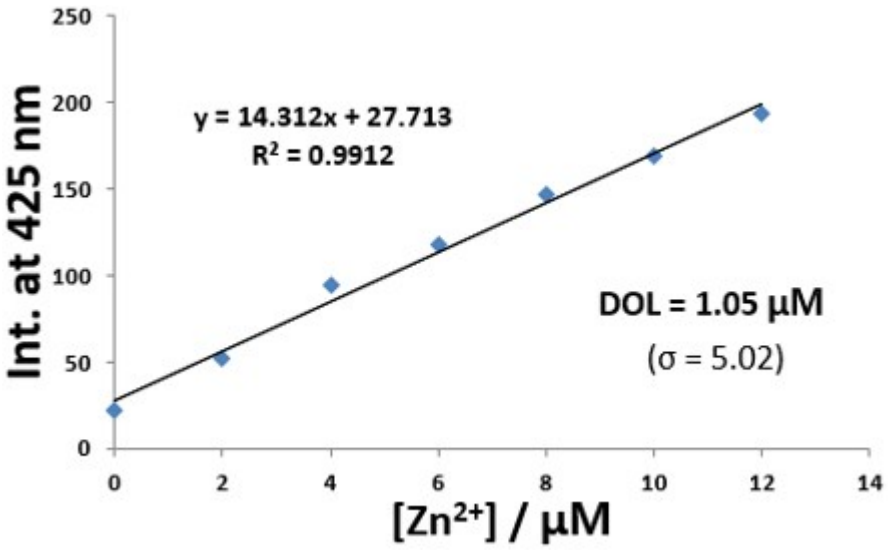

Figure S16. Determination of the detection limit based on change in the ratio (absorbance at 425 nm) of **1** (20 μM) with Zn^{2+}.

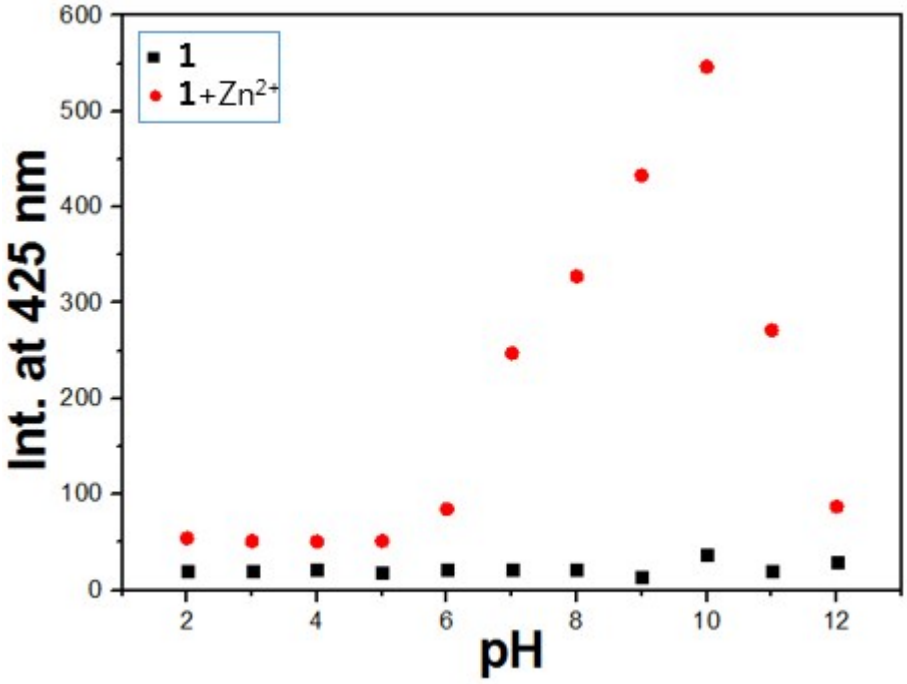

Figure S17. Fluorescence intensity of Zn^{2+}-2·**1** complex (at 425 nm) at different pH values (2-12) in DMF:bis-buffer solution (v/v, 1:1, 10 mM, pH 7.0).

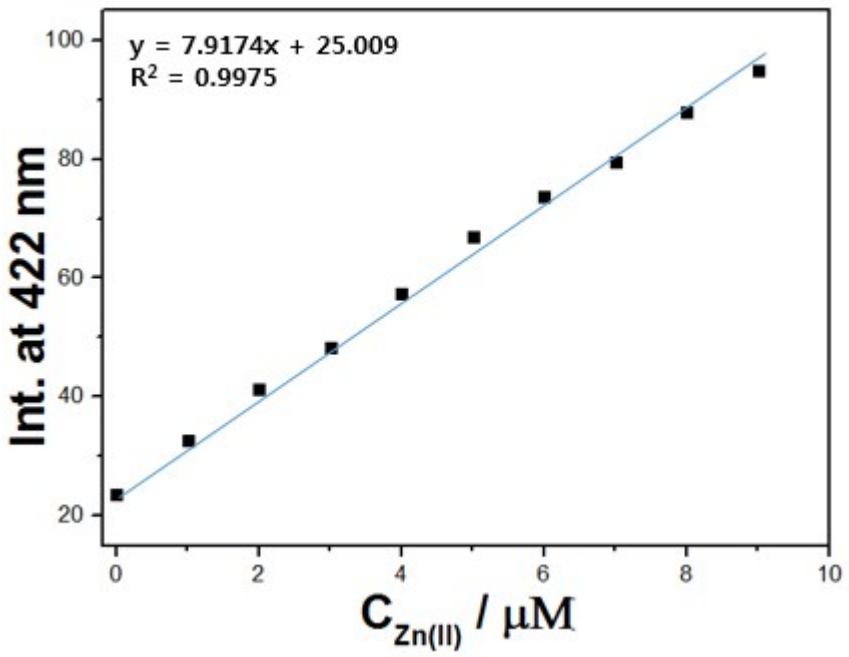

Figure S18. Fluorescence intensity (at 422 nm) of **1** as a function of Zn(II) concentration. [**1**] = 10 μmol/L and [Zn(II)] = 0.00-9.00 μmol/L. Conditions: all samples were conducted in DMF:bis-tris buffer solution (v/v, 1:1, 10 mM, pH 7.0). λ_{ex} and λ_{em} were 365 and 422 nm, respectively.

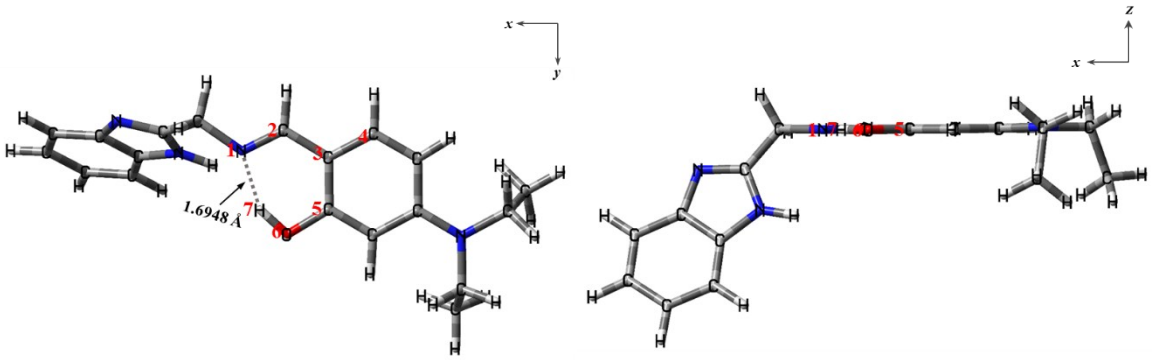

Dihedral angle (1N, 2C, 3C, 4C) : 178.806°

(a)

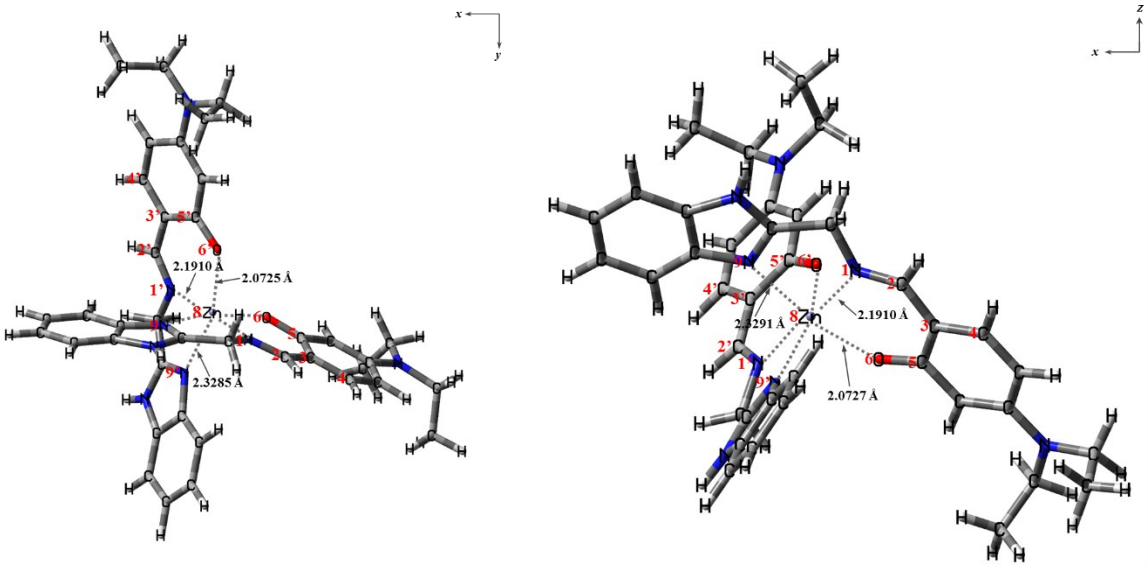

Dihedral angle (1N, 2C, 3C, 4C) : -179.009°
Dihedral angle (1'N, 2'C, 3'C, 4'C) : -179.011°

(b)

Figure S19. Energy-minimized structures of (a) **1** and (b) Zn^{2+}-2·**1** complex at B3LYP level.

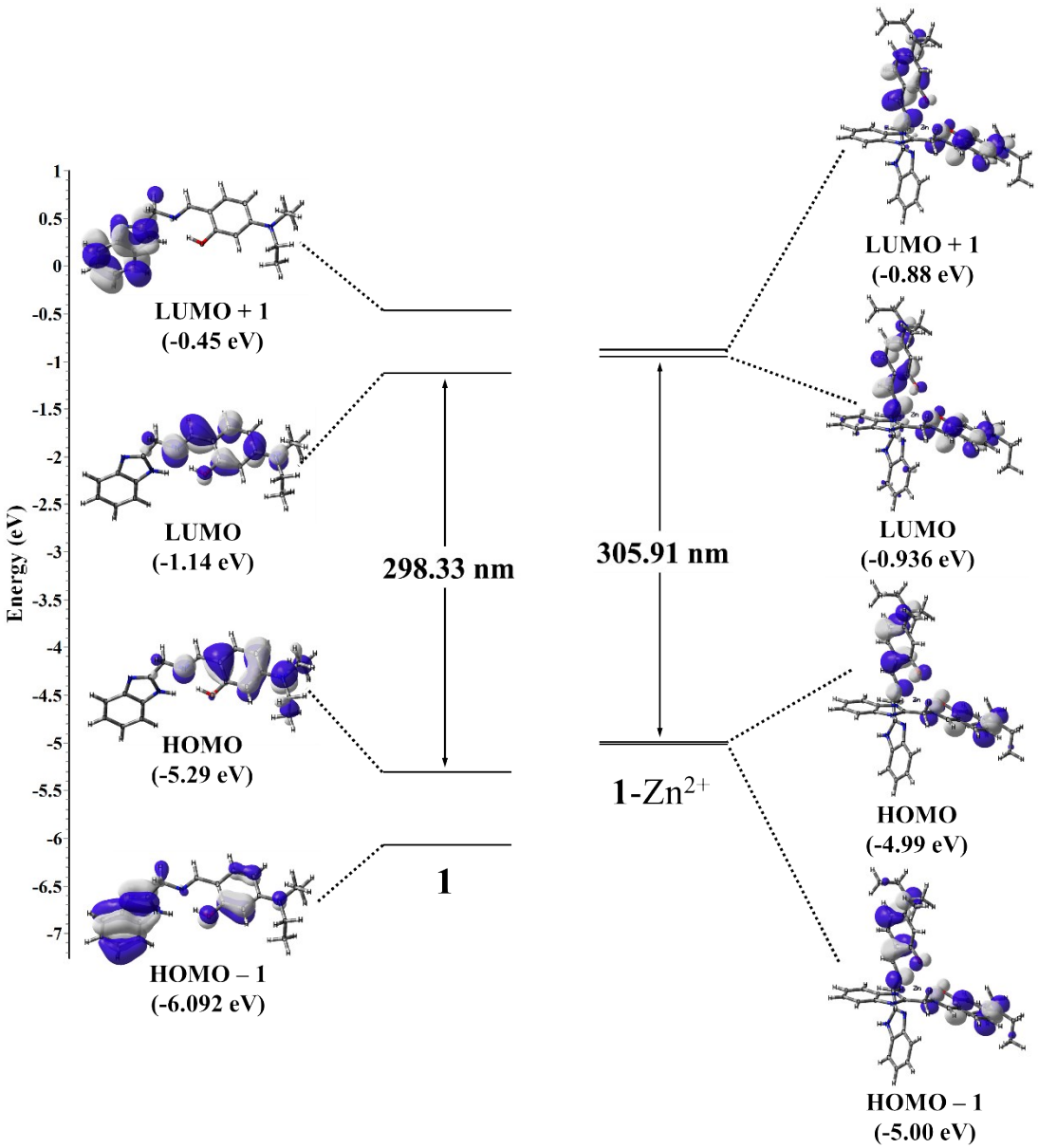

Figure S20. Molecular orbital diagrams of **1** (left) and Zn^{2+}-2·**1** (right) by DFT methods